Video Article

A Dual Tracer PET-MRI Protocol for the Quantitative Measure of Regional Brain Energy Substrates Uptake in the Rat

Maggie Roy[1], Scott Nugent[1], Sébastien Tremblay[2], Maxime Descoteaux[3], Jean-François Beaudoin[2], Luc Tremblay[2], Roger Lecomte[2,4], Stephen C Cunnane[1]

[1]Research Center on Aging and Department of Physiology and Biophysics, Université de Sherbrooke

[2]Sherbrooke Molecular Imaging Center, Étienne-Le Bel Clinical Research Center, Université de Sherbrooke

[3]Department of Computer Science, Université de Sherbrooke

[4]Department of Nuclear Medicine and Radiobiology, Université de Sherbrooke

Correspondence to: Maggie Roy at maggie.roy@usherbrooke.ca

URL: http://www.jove.com/video/50761
DOI: doi:10.3791/50761

Keywords: Neuroscience, Issue 82, positron emission tomography (PET), 18F-fluorodeoxyglucose, 11C-acetoacetate, magnetic resonance imaging (MRI), kinetic modeling, cerebral metabolic rate, rat

Date Published: 12/28/2013

Citation: Roy, M., Nugent, S., Tremblay, S., Descoteaux, M., Beaudoin, J.F., Tremblay, L., Lecomte, R., Cunnane, S.C. A Dual Tracer PET-MRI Protocol for the Quantitative Measure of Regional Brain Energy Substrates Uptake in the Rat. *J. Vis. Exp.* (82), e50761, doi:10.3791/50761 (2013).

Abstract

We present a method for comparing the uptake of the brain's two key energy substrates: glucose and ketones (acetoacetate [AcAc] in this case) in the rat. The developed method is a small-animal positron emission tomography (PET) protocol, in which ^{11}C-AcAc and ^{18}F-fluorodeoxyglucose (^{18}F-FDG) are injected sequentially in each animal. This dual tracer PET acquisition is possible because of the short half-life of ^{11}C (20.4 min). The rats also undergo a magnetic resonance imaging (MRI) acquisition seven days before the PET protocol. Prior to image analysis, PET and MRI images are coregistered to allow the measurement of regional cerebral uptake (cortex, hippocampus, striatum, and cerebellum). A quantitative measure of ^{11}C-AcAc and ^{18}F-FDG brain uptake (cerebral metabolic rate; µmol/100 g/min) is determined by kinetic modeling using the image-derived input function (IDIF) method. Our new dual tracer PET protocol is robust and flexible; the two tracers used can be replaced by different radiotracers to evaluate other processes in the brain. Moreover, our protocol is applicable to the study of brain fuel supply in multiple conditions such as normal aging and neurodegenerative pathologies such as Alzheimer's and Parkinson's diseases.

Video Link

The video component of this article can be found at http://www.jove.com/video/50761/

Introduction

Context and Rationale

Positron emission tomography (PET) enables the minimally-invasive study of functional processes in the brain. Glucose is the brain's main energy substrate, but in conditions of glucose deficiency, ketones (acetoacetate [AcAc] and β-hydroxybutyrate) are the main alternative energy substrates. Brain energy metabolism has been widely studied by PET using the most common PET tracer, ^{18}F-fluorodeoxyglucose (^{18}F-FDG), a glucose analog. Our group recently developed a novel radiotracer -^{11}C-AcAc - to measure brain ketone metabolism[1]. Magnetic resonance imaging (MRI) is a much higher resolution technique (0.1 mm × 0.1 mm in-plane resolution) than PET, and is needed to clearly localize anatomical brain regions required for the regional PET analysis of brain energy metabolism.

PET data are commonly expressed as standardized uptake values (SUV)[2-6]. SUV are the tissue activity concentration normalized by the fraction of the injected dose/unit weight, as initially proposed over 70 years ago[7]. These units are still widely used because they require simpler PET acquisition and image analysis methodologies. However, an important limitation is that SUV are relative not absolute units, making it difficult to compare results across different studies. This difficulty of comparison may contribute to contradictory findings in the literature on brain glucose uptake in the elderly[8]. Therefore, the quantitative cerebral metabolic rate (CMR; µmol/100 g/min) has particular advantages[9-11]. Generating CMR values requires a dynamic PET acquisition and the plasma radioactivity counts as a function of time, *i.e.* the plasma time-activity curve (TAC) or input function. The input function can be obtained by multiple blood samplings throughout the PET acquisition[9,12] or by the image-derived input function (IDIF) method, in which a region of interest is drawn on a blood pool (heart's left ventricle or major artery)[11,13-16].

Goal

The aim of our method was to quantitatively compare for the first time the uptake of the brain's two key energy substrates, glucose and ketones, using PET and MRI in rodents. ^{11}C-AcAc and ^{18}F-FDG were used sequentially in the same animal. The protocol was designed to measure

regional uptakes in different relevant brain structures (cortex, hippocampus, striatum, and cerebellum) clearly visible in the MR images. The protocol was also specifically intended to permit quantitative analysis of tracer brain uptake, *i.e.* CMR of both ^{18}F-FDG and ^{11}C-AcAc. Although this protocol was developed to study brain energy substrates, the radiotracers we used could be replaced by others, and the same methodology can be used to study different brain functional processes.

Advantages over existing methods

PET and MRI do not require the animal to be sacrificed after the acquisition. Therefore, follow-up studies of treatments are possible. Thus, baseline data followed by an experimental condition can be measured within the same animal, thereby reducing both biological variability and the number of animals required. A key advantage of our dual tracer PET protocol is to compare both tracers uptake in the same animal under the same physiological conditions within the same imaging session, thereby reducing even more biological variability and systematic discrepancies. This dual tracer PET protocol is feasible primarily because of the short physical half-life of ^{11}C (20.4 min) and the fast biological washout of ^{11}C-AcAc, which leave minimal residual ^{11}C radioactivity during the second acquisition with ^{18}F-FDG. The MRI scan is an important feature of this protocol as it enables the tracer uptake to be studied in specific brain areas. In addition, this method enables an absolute quantitative measure of brain tracer uptake in contrast to relative units obtained by the SUV method. Finally, ^{11}C-AcAc images have a low signal-to-noise ratio because of relatively low brain AcAc uptake under physiological conditions, which makes automatic ^{11}C-AcAc and MR images registration challenging. Hence, because ^{11}C-AcAc and ^{18}F-FDG acquisitions are sequential (no motion of the animal), the ^{18}F-FDG to MRI alignment can be applied to ^{11}C-AcAc images.

Key papers where the protocol has been used

We have used the dual tracer PET protocol in a study involving the comparison of the fasted state and the ketogenic diet (KD) in young rats[2]. We showed that both fasting and the KD increase significantly both ^{11}C-AcAc and ^{18}F-FDG brain uptake. However, these were not quantitative results as we did not use the dynamic PET imaging and tracer kinetic modeling methodology at that time. Thereafter, we undertook a regional and quantitative study of brain metabolism in aged rats, where the effect of aging and a KD were evaluated on brain ^{11}C-AcAc and ^{18}F-FDG uptake[11]. We also showed that the percentage of distribution across brain regions was different between ^{11}C-AcAc and ^{18}F-FDG. Furthermore, not only the CMR of ^{11}C-AcAc but also that of ^{18}F-FDG was increased in the whole brain as well as in the striatum of aged rats on the KD.

Protocol

All experiments were completed in accordance with the Animal Care and Use Committee at the Université de Sherbrooke and with the Canadian Council on Animal Care. The experimental protocol was approved by the Institutional Animal Research Ethics Review Board (protocol #011-09).

1. Brain Anatomy with MRI

1. Let rats acclimatize in the animal facility for a minimum of 7 days prior to the protocol. Perform brain MRI scans 1-2 weeks prior to the dual tracer PET protocol to allow full recovery from the anesthesia.
2. Anesthetize the rat in an induction chamber. Use 2% isoflurane and 1.5 L/min oxygen throughout the protocol for anesthesia. Pinch the hind leg to ensure the animal is fully anesthetized. CAUTION: inhalation of isoflurane can cause headache, dizziness, or unconsciousness in some cases; it should always be used in the presence of an air exchange system in a suitably ventilated room.
3. Position the rat on the MRI examination table in the head-first prone position with a nose cone for isoflurane. Position the respiration and rectal probes. Monitor the respiration rate during the experiment and maintain body temperature at 37 °C with an automated air warming system.
4. Acquire T_2-weighted MR images using a fast spin-echo pulse sequence with acquisition parameters as detailed previously[11]. Place the rat on a heated mat during recovery from anesthesia.

2. Dual Tracer PET Acquisitions

1. Use a small-animal PET scanner equipped with avalanche photodiode detectors, an axial field of view of ~7.5 cm and an isotropic spatial resolution of 1.2 mm[17]. Due to its short physical half-life, prepare ^{11}C by proton bombardment of natural nitrogen (through the ^{14}N(ρ,α)^{11}C nuclear reaction) in a cyclotron on-site before each experiment.
2. Fast the rat for 18 hr prior to PET scanning. Fasting allows higher brain uptake of ^{11}C-AcAc and ^{18}F-FDG, thereby improving signal-to-noise ratio.
3. Anesthetize the rat in an induction chamber. Transfer the rat onto a heating mat with a nose cone for isoflurane. Start ^{11}C-AcAc synthesis at this time. The synthesis takes 18 min from the end of bombardment, as previously described[1].
4. Position the rat on its side. Prepare a PE50 polyethylene catheter filled with heparinized 0.9% sodium chloride solution (saline). Install the catheter in the tail vein for tracer injection. Install a second catheter in the mid-ventral tail artery for blood sampling throughout the acquisitions.
5. Rapidly transfer the rat to the scanner table in the head-first prone position with a nose cone for isoflurane. Position the respiration and rectal probes. Monitor the respiration rate during the experiment and maintain body temperature at 37 °C with an automated warming air system. Move the scanner table forward into the scanner to ensure the appropriate imaging of the brain and the heart simultaneously. As an anatomical landmark, position the edge of the field of view on the rat's eyes (with the help of laser lines).

6. Using a concentrated ^{11}C-AcAc solution (~1 GBq/ml), prepare a syringe of ~50 MBq of radioactivity (a range of 45-55 MBq is acceptable). Adjust the volume to 300 µl with saline. CAUTION: Radioactivity can be harmful for the health. It should always be handled behind a lead shield. The experimenter should be wearing a body and ring dosimeter. A Geiger counter should also be on during the experiment.
7. Install the syringe on an injection pump. Start the bolus injection of ^{11}C-AcAc at a rate of 1 ml/min (injection duration: ~19 sec). On a second pump, immediately after terminating the ^{11}C-AcAc injection, start the injection of 300 µl of saline at a rate of 1 ml/min, which is important for an optimal injection of tracer into the blood circulation.
8. Start a dynamic PET data acquisition 30 sec before starting the bolus injection for a total duration of 20.5 min. The 30 sec data acquisition before the tracer injection provides a measure of the ambient background to be subsequently subtracted from the PET data. Set the regular sampling mode and the energy window at 250-650 keV.
9. Collect two 200 µl blood samples at ~15 and 18 min after starting the ^{11}C-AcAc injection. Inject heparinized saline in the catheter after each sampling to avoid blood clotting. Take note of the time at the beginning and the end of blood sampling and use the mean time. Centrifuge at 6,000 RPM for 5 min and collect plasma. Measure radioactivity counts in plasma using a gamma counter calibrated with the PET scanner.
10. After the ^{11}C-AcAc scan, allow a waiting period of 20 min to ensure that most of radioactivity has decayed. The period can vary from 15-30 min. Do not move the scanner bed and leave the rat under isoflurane throughout this period.
11. During this time, using a concentrated ^{18}F-FDG solution (~5.5 GBq/µl), prepare a syringe of ~50 MBq. Proceed exactly as mentioned in steps 2.6 and 2.7. Start a dynamic acquisition of a total duration of 40.5 min, including the 30 sec before the injection. Collect two 200 µl blood samples at ~30 and 35 min after starting the ^{18}F-FDG injection.
12. At the end of the ^{18}F-FDG acquisition, take one final 200 µl blood sample. Centrifuge and collect plasma. Keep plasma samples at -80 °C for glucose and AcAc analysis.
13. Finally, place the rat on a heating mat during the waking period. Keep the animal for a longitudinal follow-up, or alternatively, euthanize the rat for brain sampling and further biochemical studies.
14. Reconstruct the PET images according to the following time frame sequences: 1 × 30 sec; 12 × 5 sec; 8 × 30 sec; and n × 300 sec, where n = 3 for ^{11}C-AcAc acquisition and n = 7 for ^{18}F-FDG acquisition.

3. Plasma Glucose and AcAc Analysis

1. Measure plasma glucose and AcAc with a clinical chemistry analyzer. Perform assays within 48 hr of the blood sampling to minimize AcAc decarboxylation into acetone. Measure glucose concentration with DF40 kit as previously described[18] and AcAc with an open channel[2]. This type of analyzer is more accurate than strips (0.1 µM) and has a broad detection window.

4. Quantitative PET Analysis

1. Use *PMOD* software or an equivalent system for small-animal PET image analysis.
2. Plasma time-activity curve (TAC)
    1. Load ^{18}F-FDG data. Sum image frames of the first 60 sec following injection (when tracer is mainly in blood).
    2. Using a manual drawing tool, draw a volume of interest (VOI) on the left ventricular cavity blood pool (a large pool centered in the bottom part of images). Draw the VOI ~1 mm inside of the edge of the blood pool (red voxels) to ensure no inclusion of tissue and avoid tissue radioactivity spill into the blood pool (**Figure 1A**). Copy the VOI to the entire dynamic image series and generate a curve of radioactivity as a function of time (TAC).
    3. In a spreadsheet, use radioactivity counts of the two plasma samples taken during the acquisition to correct plasma TAC (**Figure 1B**). Use the following equation:

$$IDIFcorrected(t) = \frac{IDIF(t)}{correction}, correction = \frac{1}{2}\left(\frac{IDIF(t_n)}{plasma1} + \frac{IDIF(t_{n+1})}{plasma2}\right)$$

    Some smoothing of the plasma TAC can be performed.
    4. Verify if residual radioactivity from ^{11}C-AcAc is present in the first 30 sec of ^{18}F-FDG scan, prior to injection. If so, subtract the following factor from all the subsequent time frames of the TAC:

$$R \times e^{-\left(\frac{\ln 2}{t_{1/2}}\right) \times T},$$

    where R is the residual radioactivity, $t_{1/2}$ is the half-life of ^{11}C (20.4 min) and T is the time frame[2,13]. Residual radioactivity from ^{11}C-AcAc after a waiting period of 20 min can be up to 1.5% of maximal ^{18}F-FDG counts.

3. ^{18}F-FDG/MRI coregistration
    1. Apply coregistration obtained with ^{18}F-FDG images to the ^{11}C-AcAc images. This is necessary because ^{11}C-AcAc images have a low signal-to-noise ratio and automatic coregistration is difficult.
    2. Load the corresponding MRI data. Load all 28 ^{18}F-FDG time frames in the same orientation as the MR images (on three axes).

3. Compute the ^{18}F-FDG summed image of the 28 time frames. This generates an image with higher counts, so it is easier to work with for coregistration with MRI than individual image frames.
4. Perform the automatic coregistration of the ^{18}F-FDG summed image on MR images (**Figure 2**). Apply the transformation to all individual ^{18}F-FDG image frames. Save the transformation which will later be applied to ^{11}C-AcAc images.

4. Volumes of interest (VOIs)
   1. Using segmentation software such as *PMOD*, select MRI data and choose preferred plane for manual drawing. Choose the manual or the semi-automatic drawing tool, depending on brain region size and image contrast. Locate brain structures according to a standard rat brain atlas[19].
   2. Draw the VOIs. As shown in **Figure 3**, segment the whole brain, cortex, hippocampus, striatum and cerebellum, but other regions could be chosen. Save the VOIs, which will be applied to the coregistered ^{18}F-FDG and ^{11}C-AcAc images.
   3. Apply VOIs to ^{18}F-FDG coregistered images. Select the VOI statistics to visualize brain TAC. If needed, correct TAC by subtracting the decay-corrected mean radioactivity in the first 30 sec from all the subsequent time frames.

5. Cerebral metabolic rate calculation
   1. Load brain and the corresponding plasma TACs.
   2. Select Patlak plot kinetic model[20,21]. Set the lumped constant to 0.48[22] and the corresponding plasma glucose concentration (**Figure 4B**). Set the maximal relative deviation from the Patlak plot to 5%. Fit the data to the model.

6. ^{11}C-AcAc images
   1. Compute the ^{18}F-FDG summed image of the 24 first time frames to have the same number of frames as the ^{11}C-AcAc scan. Otherwise, ^{11}C-AcAc/MRI coregistration fails. Perform the automatic coregistration of ^{18}F-FDG on MRI. Save the transformation process which will be used for ^{11}C-AcAc image coregistration.
   2. Repeat steps 4.2 and 4.3 for ^{11}C-AcAc images. Use ^{18}F-FDG transformation in step 4.6.1 and apply it to all individual ^{11}C-AcAc image frames. Repeat steps 4.4 and 4.5 and use ^{18}F-FDG saved VOIs. Set the lumped constant to 1.

Representative Results

As seen in **Figure 2**,^{11}C-AcAc uptake is low within the brain itself. As mentioned earlier, ketones consumption by the brain is very low on a short-term fasting. ^{11}C-AcAc uptake is higher in the tongue and cheek muscles. Indeed, ketones are rapidly taken up by rat skeletal muscles[23]. In contrast, ^{18}F-FDG uptake is mostly in the brain and the cheek muscles. **Figure 2** shows that during the coregistration process, MR images are fixed and PET images move due to an alignment in the axial plane.

We use the Patlak kinetic model[20,21] to determine brain uptake, which has been previously used for ^{11}C-ketone and ^{18}F-FDG kinetic modeling[9,12,24,25]. This model uses equation 1, where the measured PET activity (C_{Tissue}) is divided by plasma activity (C_P) and plotted at a normalized time. The variable *K* represents brain influx and *V* is the tracers distribution volume. After brain uptake steady state is achieved, the curve results in a straight line (**Figure 4A**). The slope represents brain influx (*K*). Typical values of brain influx (*K*) and distribution volume (*V*) in the whole brain for ^{18}F-FDG are ~0.0165 min^{-1} and ~0.6425 ml blood/ml tissue, respectively (**Figure 4B**). As for ^{11}C-AcAc, typical values are ~0.0325 min^{-1} and ~0.5315 ml blood/ml tissue.

$$\frac{C_{Tissue}(t)}{C_P(t)} = K\frac{\int_0^t (C_P(t)dt)}{C_P(t)} + V \quad (1)$$

Cerebral metabolic rate of glucose (CMR_{glc}) and AcAc (CMR_{AcAc}) are calculated according to equations 2 and 3. Brain influx and plasma concentrations are required. For CMR_{glc}, the lumped constant (LC) is used to convert ^{18}F-FDG uptake to glucose uptake. We use a LC value of 0.48, as previously reported in rats[22]. No constant is used for CMR_{AcAc} calculation as the radiotracer has the exact same chemical formula as the endogenous molecule.

$$CMR_{glc} = \frac{K*[glucose]}{LC} \quad (2)$$

$$CMR_{AcAc} = K * [AcAc] \quad (3)$$

One can expect whole brain CMR_{glc} and CMR_{AcAc} of approximately 24 µmol/100 g/min and 3 µmol/100 g/min, respectively, in healthy adult rats fasted for 18 hr prior the PET acquisitions[11]. In the rat, CMR_{AcAc} is therefore about 12% of that of CMR_{glc}.

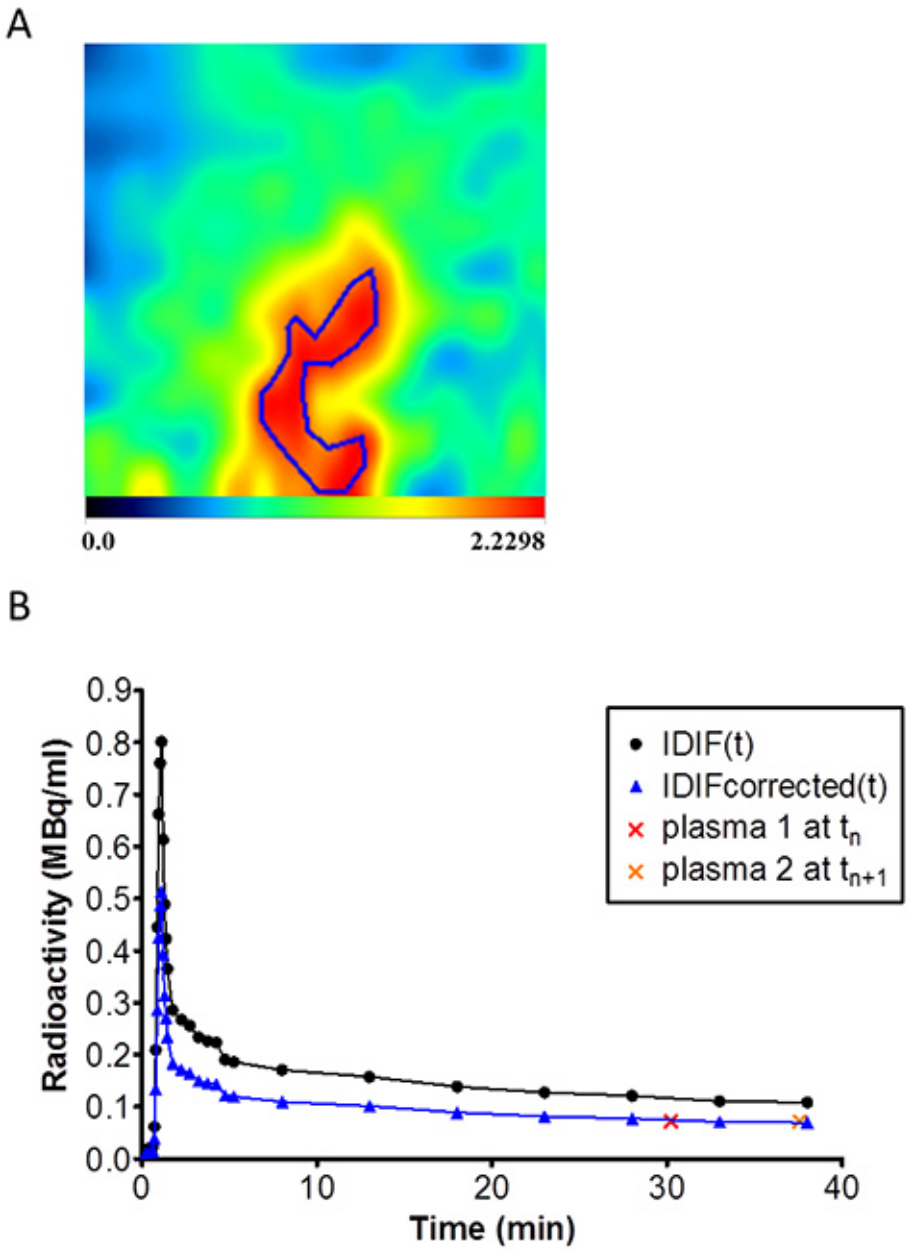

Figure 1. Plasma time-activity curve (TAC) assessment. A) Volume of interest drawn on the blood pool in the left ventricle of the heart using a manual drawing tool. This is a ^{18}F-FDG image showing the average radioactivity for the first 60 sec after the injection. **B**) ^{18}F-FDG plasma TAC obtained by image-derived input function (IDIF; black), the two plasma samples collected 30 min (red) and 37.5 min (orange) after the injection and ^{18}F-FDG plasma TAC after correction with radioactivity counts of the two plasma samples (blue). Click here to view larger image.

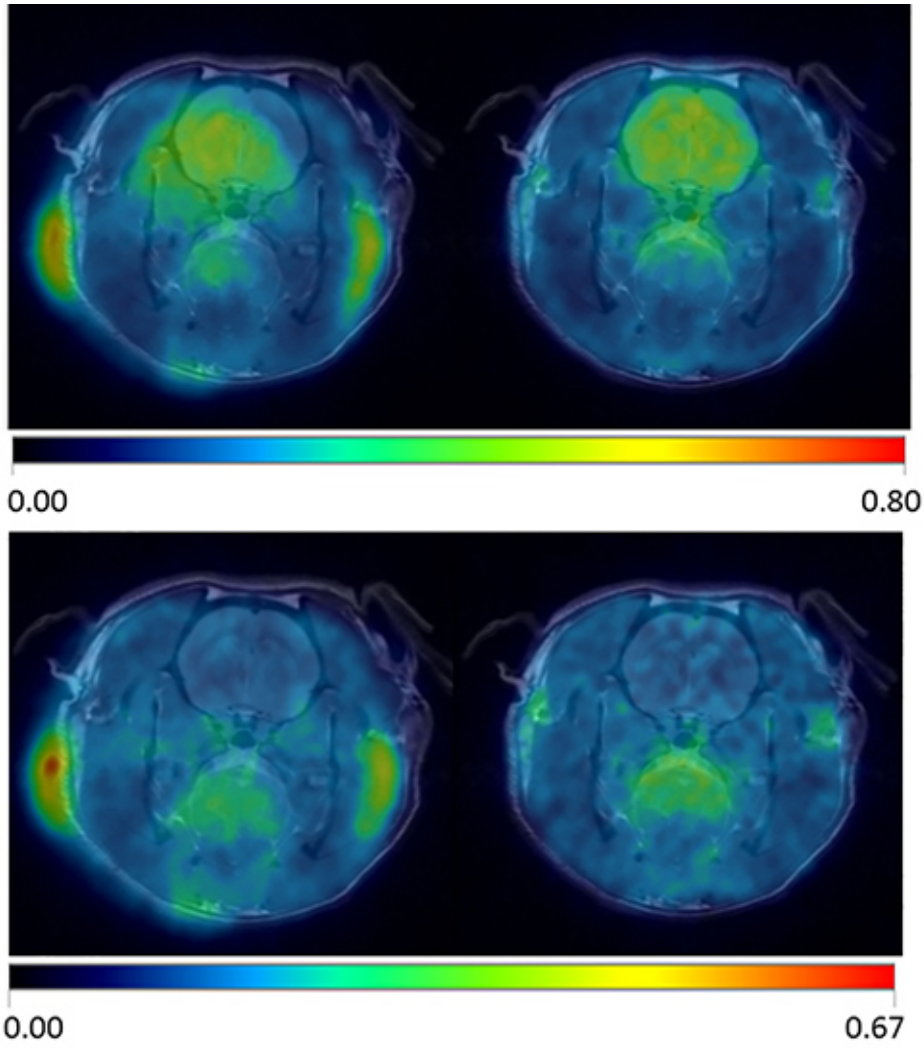

Figure 2. PET/MRI automatic coregistration process. Axial PET and MR images before (left) and after (right) automatic coregistration with *PMOD* software. ^{18}F-FDG (top) and ^{11}C-AcAc (bottom) images are shown. ^{11}C-AcAc/MRI coregistration is performed using the ^{18}F-FDG/MRI transformation parameters. Click here to view larger image.

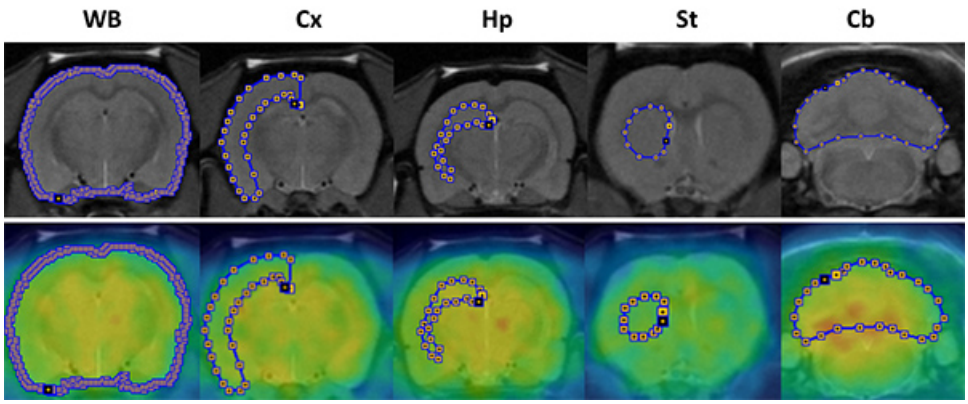

Figure 3. Volumes of interest (VOIs) drawing. VOIs drawn on axial MR images (top). VOIs applied to ^{18}F-FDG coregistered images (bottom). WB: whole brain; Cx: cortex; Hp: hippocampus; St: striatum; Cb: cerebellum. Click here to view larger image.

A

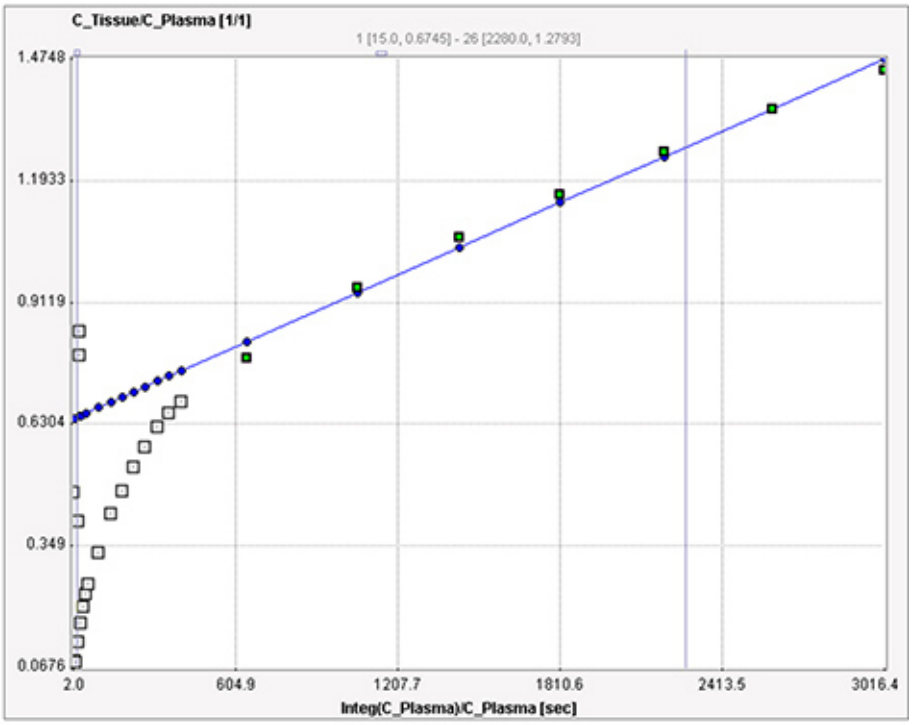

B

Parameter	Current value	Unit	% SE
Lumped Constant	0.48	1/1	
Plasma Gluc.	8.3	mmol/l	
✔ t*	5.5	min	---
Max. Err.	5.0	%	
MRGlu.	27.523023	µmol/min/100g	4.43
Slope	0.016554	ml/ccm/min	4.43
Intercept	0.64257	norm. act.	3.78
Start	10.818252	norm. min.	---
ChiSquared	0.003204		

Figure 4. Kinetic modeling of brain ^{18}F-FDG uptake using *PMOD* software. A) Patlak plot of ^{18}F-FDG uptake in the whole brain. Y-axis correspond to the measured PET activity (C_{Tissue}) divided by plasma activity (C_P) and x-axis correspond to the normalized time. The curve results in a straight line once steady state is reached. The slope represents brain influx (*K*). **B**) Cerebral metabolic rate of glucose (*MRGlu.*) and plot parameters of the corresponding ^{18}F-FDG acquisition, where *Plasma Gluc.* is the plasma glucose concentration, *Max. Err.* is the maximal relative deviation from the Patlak regression line, *Slope* is the brain influx (*K*) and *Intercept* is the distribution volume (*V*). Click here to view larger image.

Discussion

Critical steps

A critical step in this dual tracer PET protocol is to be able to simultaneously scan the heart's left ventricle and the brain at the same time. This requires a PET scanner with a sufficient axial length, *i.e.* a minimum of 7.5 cm. A few test scans are needed to determine the exact position of the scanner table (x, y, and z values), where the brain and the heart are scanned correctly.

Tracer injection is also a crucial point for a successful PET acquisition. The catheter must be correctly inserted in the vein. Heparinized saline solution should flow into the vein smoothly without blood clotting. For a quantitative measure of brain uptake, an accurate plasma TAC is essential. When drawing the VOI on blood in the left ventricle, it is important to include the fewest possible tissue pixels. Blood samples are also crucial to correct the plasma TAC derived from the PET images. Indeed, as seen in **Figure 1B**, radioactivity in plasma samples may be different than in the IDIF. This is due to the spill-in effect in the last time frames (contamination of blood by radiation in adjacent tissues)[26], which affects the IDIF. The brain MR image is essential for regional brain analysis. After the coregistration process, the alignment of PET and MR images of every brain slice should be verified to ensure that the subsequent PET regional brain analysis is accurate. Finally, a good fit of data to the Patlak plot is required for accurate calculation of CMR. Data should be as linear as possible; if not, the plasma and brain TAC should be rechecked.

Limitations

A significant limitation of PET imaging is that it provides no information on the chemical status of the radiotracer, *i.e.* degradation to other metabolites in the brain. Indeed, ^{18}F-FDG is taken up by brain cells, where it is trapped as ^{18}F-FDG-6-phosphate. This contrasts with nuclear magnetic resonance spectroscopy (NMRS) where the labeled atom can be monitored in multiple metabolic pathways[27-29]. However, PET requires very low amounts of radiotracer (10^{-12}-10^{-9} M) compared to NMRS, and therefore better reflects physiological conditions. Another limitation comes from the plasma TAC derived from the PET images, which can be inexact because of the spill-out effect from blood to tissues in the first time frames[26]. Indeed, the present method does not include blood sampling in the first time frames. When drawing the VOI in the left ventricle, heart tissue may be included in the VOI without noticing because of heart beat, which may affect the plasma TAC. Indeed, the present method does not include electrocardiogram-gated PET acquisitions. The multiple blood sampling method is the gold standard for the most accurate plasma TAC, but remains demanding and invasive for small animals. Indeed, this technique would require approximately 18 blood samplings per scan for both scan, which would represent a considerable volume of blood sampled. Finally, for ^{11}C-AcAc acquisitions, no correction for loss of ^{11}C-CO_2 from the tissue is performed. However, previous ^{11}C-ketone PET studies showed that loss of ^{11}C-CO_2 had minimal impact on data, since the Patlak plot was well described by a straight line, and did not correct data for this loss[24,25].

Possible modifications

This protocol is also applicable for the study of mice models. Fasting can be shortened to 6 hr prior to the PET scan. However, with less than 6 hr, ^{11}C-AcAc brain uptake will not be high enough for accurate CMR computation. Indeed, the brain consumes more ketones as the fasting period is prolonged. We have previously shown that after a 48 hr fasting, brain ^{11}C-AcAc uptake increases by 160% and that brain ^{18}F-FDG uptake also increases by 277%[2]. Electrocardiogram-gated PET acquisitions can be performed and may enable a more accurate plasma TAC. One can use another type of anesthetic such as propofol or ketamine depending of the Institutional Animal Care and Use guidelines. If an injection of anesthetic needs to be done during the dual PET tracer protocol, it should be performed between the two scans and attention should be paid not to move the animal. A longer delay is also possible between the two PET scans to reduce residual radioactivity from ^{11}C in the ^{18}F-FDG scan. However, the total period for anesthesia should be kept as short as possible since anesthesia decreases brain metabolism[30]. For quantitative PET analysis, any custom software enabling coregistration process and kinetic modeling can be used. If the automatic PET-MRI coregistration process is not possible, the registration can be performed manually. It is however a longer process and prone to human error. Finally, the two-tissue compartment kinetic model is also a good model for ^{18}F-FDG brain uptake analysis and has been previously used in animal PET studies[10,12]. As for ^{11}C-AcAc, the one and two-tissue compartment models were shown to give identical results as the Patlak model[24,25].

Significance of the method

The presented method permits sequential measurement of regional brain uptake of two PET tracers and, hence, their comparison in the same animal under the same conditions. Therefore, this protocol is ideal for comparative studies of brain metabolic pathways using these PET tracers. Since the animals recover from the procedure, it can be repeated after an experimental intervention. This method also enables the absolute quantitative assessment of cerebral metabolic rates (µmol/100 g/min) in contrast to relative data obtained by the SUV method.

Future applications

The investigation of brain ketone and glucose metabolism using ^{11}C-AcAc and ^{18}F-FDG uptake by PET is relevant in many physiological and pathological processes such as aging, neurodegenerative patterns and tumor expansion or treatment. Other PET tracers can be studied with the present protocol: ^{11}C-palmitate and ^{18}F-fluorothioheptadecanoic acid uptake can be used to evaluate fatty acids esterification in conditions such as aging or type 2 diabetes. ^{11}C-Pittsburgh Compound-B, which binds fibrillar amyloid-β plaques, could potentially be used in conjunction with ^{18}F-FDG for the study of Alzheimer-like brain pathologies. Furthermore, ^{18}F-fluorodopamine is useful to evaluate dopamine circuits in disease such as Parkinson. This dual tracer PET and MRI protocol can be applied to the study of other organs such as the liver, heart, kidney, or tumors.

Disclosures

The authors declare that they have no competing financial interests.

Acknowledgements

This study was financially supported by the Fonds de la recherche en santé du Québec, Canadian Institutes of Health Research, Canadian Foundation for Innovation and the Canada Research Chairs Secretariat (SCC). The Sherbrooke Molecular Imaging Center is part of the FRQS-funded Étienne-Le Bel Clinical Research Center. The authors thank Mélanie Fortier, Jennifer Tremblay-Mercier, Alexandre Courchesne-Loyer, Dr. Fabien Pifferi, Dr. M'hamed Bentourkia, Dr. Otman Sarrhini, Dr. Jacques Rousseau, Caroline Mathieu, and Mélanie Archambault for generous support and technical assistance. The authors would like to thank the image analysis and visualization platform (http://pavi.dinf.usherbrooke.ca) for their help.

References

1. Tremblay, S., *et al.* Automated synthesis of ^{11}C-acetoacetic acid, a key alternate brain fuel to glucose. *Appl. Radiat. Isot.* **65**, 934-940, doi:10.1016/j.apradiso.2007.03.015 (2007).
2. Pifferi, F., *et al.* Mild experimental ketosis increases brain uptake of ^{11}C-acetoacetate and ^{18}F-fluorodeoxyglucose: a dual-tracer PET imaging study in rats. *Nutr. Neurosci.* **14**, 51-58, doi:10.1179/1476830510Y.0000000001 (2011).
3. Lopez-Grueso, R., Borras, C., Gambiniy, J. & Vina, J. El envejecimiento y la ovariectomia causan una disminucion del consumo cerebral de glucosa *in vivo* en ratas Wistar. *Revista Espanola de Geriatria y Gerontologia*. **45**, 136-140 (2010).
4. Fueger, B. J., *et al.* Impact of animal handling on the results of ^{18}F-FDG PET studies in mice. *J. Nucl. Med.* **47**, 999-1006 (2006).
5. Luo, F., *et al.* Characterization of 7- and 19-month-old Tg2576 mice using multimodal *in vivo* imaging: limitations as a translatable model of Alzheimer's disease. *Neurobiol. Aging.* **33**, 933-944, doi:10.1016/j.neurobiolaging.2010.08.005 (2012).
6. Poisnel, G., *et al.* Increased regional cerebral glucose uptake in an APP/PS1 model of Alzheimer's disease. *Neurobiol. Aging.* **33**, 1995-2005, doi:10.1016/j.neurobiolaging.2011.09.026 (2012).
7. Kenney, J. M., Marinelli, L. D. & Woodard, H. Q. Tracer studies with radioactive phosphorus in malignant neoplastic disease. *Radiology.* **37**, 683-690 (1941).
8. Cunnane, S., *et al.* Brain fuel metabolism, aging, and Alzheimer's disease. *Nutrition*. **27**, 3-20, doi:10.1016/j.nut.2010.07.021 (2011).
9. Shimoji, K., *et al.* Measurement of cerebral glucose metabolic rates in the anesthetized rat by dynamic scanning with ^{18}F-FDG, the ATLAS small animal PET scanner, and arterial blood sampling. *J. Nucl. Med.* **45**, 665-672 (2004).
10. Tantawy, M. N., & Peterson, T. E. Simplified [^{18}F]FDG image-derived input function using the left ventricle, liver, and one venous blood sample. *Mol. Imaging*. **9**, 76-86 (2010).
11. Roy, M., *et al.* The ketogenic diet increases brain glucose and ketone uptake in aged rats: A dual tracer PET and volumetric MRI study. *Brain Res.* doi:10.1016/j.brainres.2012.10.008 (2012).
12. Yu, A. S., Lin, H. D., Huang, S. C., Phelps, M. E., & Wu, H. M. Quantification of cerebral glucose metabolic rate in mice using ^{18}F-FDG and small-animal PET. *J. Nucl. Med.* **50**, 966-973, doi:jnumed.108.060533 [pii]10.2967/jnumed.108.060533 (2009).
13. Bentourkia, M., *et al.* PET study of ^{11}C-acetoacetate kinetics in rat brain during dietary treatments affecting ketosis. *Am. J. Physiol. Endocrinol. Metab.* **296**, E796-801, doi:10.1152/ajpendo.90644.2008 (2009).
14. Menard, S. L., *et al.* Abnormal *in vivo* myocardial energy substrate uptake in diet-induced type 2 diabetic cardiomyopathy in rats. *Am. J. Physiol. Endocrinol. Metab.* **298**, E1049-1057, doi:10.1152/ajpendo.00560.2009 (2010).
15. Liistro, T., *et al.* Brain glucose overexposure and lack of acute metabolic flexibility in obesity and type 2 diabetes: a PET-[^{18}F]FDG study in Zucker and ZDF rats. *J. Cereb. Blood Flow Metab.* **30**, 895-899, doi:10.1038/jcbfm.2010.27 (2010).
16. Croteau, E., *et al.* Image-derived input function in dynamic human PET/CT: methodology and validation with ^{11}C-acetate and ^{18}F-fluorothioheptadecanoic acid in muscle and 18F-fluorodeoxyglucose in brain. *Eur. J. Nucl. Med. Mol. Imaging*. **37**, 1539-1550, doi:10.1007/s00259-010-1443-z (2010).
17. Bergeron, M., Cadorette, J. & Beaudoin, J. F. Performance evaluation of the LabPETTM APD-based digital PET scanner. *IEEE Trans. Nucl. Sci.* **56**, 10-16 (2009).
18. Freemantle, E., *et al.* Metabolic response to a ketogenic breakfast in the healthy elderly. *J. Nutr. Health Aging*. **13**, 293-298 (2009).
19. Paxinos, G., & Watson, C. *The rat brain in stereotaxic coordinates*. sixth edn, Elsevier (2007).
20. Patlak, C. S., Blasberg, R. G., & Fenstermacher, J. D. Graphical evaluation of blood-to-brain transfer constants from multiple-time uptake data. *J. Cereb. Blood Flow Metab.* **3**, 1-7, doi:10.1038/jcbfm.1983.1 (1983).
21. Patlak, C. S., & Blasberg, R. G. Graphical evaluation of blood-to-brain transfer constants from multiple-time uptake data. Generalizations. *J. Cereb. Blood Flow Metab.* **5**, 584-590, doi:10.1038/jcbfm.1985.87 (1985).
22. Sokoloff, L., *et al.* The ^{14}C deoxyglucose method for the measurement of local cerebral glucose utilization: theory, procedure, and normal values in the conscious and anesthetized albino rat. *J. Neurochem.* **28**, 897-916 (1977).
23. Robinson, A. M.. & Williamson, D. H. Physiological roles of ketone bodies as substrates and signals in mammalian tissues. *Physiol Rev.* **60**, 143-187 (1980).
24. Blomqvist, G., *et al.* Use of R-beta-[$^{1\text{-}11}$C]hydroxybutyrate in PET studies of regional cerebral uptake of ketone bodies in humans. *Am. J. Physiol.* **269**, E948-959 (1995).
25. Blomqvist, G., *et al.* Effect of acute hyperketonemia on the cerebral uptake of ketone bodies in nondiabetic subjects and IDDM patients. *Am. J. Physiol. Endocrinol. Metab.* **283**, E20-28, doi:10.1152/ajpendo.00294.2001 (2002).
26. Soret, M., Bacharach, S. L., & Buvat, I. Partial-volume effect in PET tumor imaging. *J. Nucl. Med.* **48**, 932-945, doi:10.2967/jnumed.106.035774 (2007).
27. Jiang, L., Mason, G. F., Rothman, D. L., de Graaf, R. A., & Behar, K. L. Cortical substrate oxidation during hyperketonemia in the fasted anesthetized rat *in vivo*. *J. Cereb. Blood Flow Metab.* **31**, 2313-2323, doi:10.1038/jcbfm.2011.91 (2011).
28. Melo, T. M., Nehlig, A., & Sonnewald, U. Neuronal-glial interactions in rats fed a ketogenic diet. *Neurochem. Int.* **48**, 498-507, doi:10.1016/j.neuint.2005.12.037 (2006).
29. Yudkoff, M., *et al.* Response of brain amino acid metabolism to ketosis. *Neurochem. Int.* **47**, 119-128, doi:10.1016/j.neuint.2005.04.014 (2005).
30. Matsumura, A., *et al.* Assessment of microPET performance in analyzing the rat brain under different types of anesthesia: comparison between quantitative data obtained with microPET and *ex vivo* autoradiography. *Neuroimage*. **20**, 2040-2050 (2003).

